Bull Earthquake Eng (2016) 14:161–184
DOI 10.1007/s10518-015-9818-y

ORIGINAL RESEARCH PAPER

An improved complex multiple-support response spectrum method for the non-classically damped linear system with coupled damping

Guohuan Liu[1,2] · Jijian Lian[1,2] · Chao Liang[1,2] · Gang Li[3] · Jinjun Hu[4]

Received: 31 March 2015 / Accepted: 13 September 2015 / Published online: 22 September 2015

Abstract An improved complex multiple-support response spectrum (CMSRS) method considering the coupled damping, which is ignored in conventional CMSRS method, is proposed in this article. Due to the nonorthogonality of the damping matrix, the complex mode analysis method is adopted for equation decoupling. Nine new cross-correlation coefficients are introduced into the CMSRS formulae, thus the correlations between the modal responses under different excitations (velocity or acceleration) are comprehensively considered. A typical structure equipped with concentrated or coupled damper is taken as example to illustrate the differences between the conventional and improved CMSRS methods. Numerical results indicate that, for the structure equipped with the concentrated damper, the coupled damping has a minor effect on the dynamic response. However, for the structure equipped with the coupled damper, the relative deviation between the responses calculated by the two methods increases with increasing damping. The maximum relative deviation of displacement even exceeds 20 %. Therefore, it is significant to consider the coupled damping in seismic engineering.

Keywords Non-classical damping system · Multiple-support excitations · Response spectrum method · Complex mode superposition method · Coupled damping

✉ Guohuan Liu
liugh@tju.edu.cn

[1] State Key Laboratory of Hydraulic Engineering Simulation and Safety, Tianjin University, 300072 Tianjin, China

[2] School of Civil Engineering, Tianjin University, 300072 Tianjin, China

[3] Faculty of Infrastructure Engineering, Dalian University of Technology, 116024 Dalian, Liaoning Province, China

[4] Institute of Engineering Mechanics, China Earthquake Administration, 150080 Harbin, Heilongjiang Province, China

1 Introduction

In structural seismic design, response spectrum method is widely adopted in many existing building codes and specifications. However, the traditional response spectrum method is developed on the basis of uniform earthquake excitation and is inapplicable for the long-span structures subjected to multiple-support excitations. Several investigators extended the response spectrum method for the case of multiple-support excitations. Rutenberg and Heidebrecht (1987) proposed a simple and approximate response spectrum technique for the multiple-support excitations problem. Yamamura and Tanaka (1990) studied the response of flexible multi-degree-of-freedom systems under multiple-support excitations by dividing the ground motion of the supports into independent subgroups. The coherency effect is included in the response spectrum analysis by Berrah and Kausel (1992) for the structures subjected to spatially varying motion. Kiureghian and Neumnhofer (1992) developed a responses spectrum method for multiple-support excitations using the principles of random vibration for classically damped linear system. Lou and Ku (1995) proposed a response spectrum method for the seismic analysis of a multiple-support structure subjected to spatially varying ground motions. The large-span structure seismic response has been analyzed in Kato's papers (Kato and Su 2002; Kato et al. 2003) considering the input difference, wave passage effect and local site effect. Song et al. (2007) presented a transformation approach for relatively accurate and rapid determination of the maximum peak responses of a linear structure subjected to three-dimensional excitations within all possible seismic incident angles. Alexander (2008) used real multi-station data from SMART-1 to generate a more detailed picture of the spatial heterogeneity. Liang and Lee (2013) suggested a methodology to estimate the structural dynamic response considering regular time invariant loads as well as extreme loads, which are time variable.

Based on the theoretical investigation, different kinds of structures, e.g., rigid plate (Hao 1991), symmetric and asymmetric structures (Hao and Xiao 1995, 1996), cable-stayed bridge (Allam and Datta 2000), multilayer architecture (Heredia-Zavoni and Leyva 2003), two-line-support large space structure (Su et al. 2006) and train-bridge system (Zhang et al. 2010), and so on, are taken as examples to calculate their dynamic responses under multiple-support seismic excitations.

Recently, the dynamic analysis of non-classically damped linear systems attracts much attention, because many non-uniform damping problems are involved in practical structure analysis, e.g., soil-structure interaction system, structures equipped with supplemental dampers and structures composed of materials with different damping. For a non-classically damped linear system, the traditional mode superposition method fails due to the nonorthogonality of the damping matrix. A modal decomposition procedure based on the complex eigenvectors and eigenvalues of the system is used by Igusa et al. (1984) to derive general expressions for spectral moments of response. Maldonado and Singh (1991) presented a response spectrum method which combines the analytical advantage of the mode acceleration formulation and the practical advantage of the mode displacement formulation for seismic response calculation of non-classically damped structures. Constantinou and Symans (1992) studied earthquake dynamic responses of the one-story and three-story steel structures both with and without fluid viscous dampers. Results show that the addition of supplemental dampers significantly reduces the response of the structure in terms of both interstory drifts and shear forces. Moreover, the comparison between the experimental responses and the analytical results show very good agreement. In order to get practical conditions of structural controllability, two necessary conditions of controllability of a repeated eigenvalues system (regular and defective system) and their proofs are given by

Yao and Gao (2011). Zhou et al. (2004, 2008; Yu et al. 2012) developed the CMSRS method for seismic analysis of non-classically damped linear system subjected to spatially varying multiple-support ground motions.

It is debatable whether the coupled damping of non-classically damped linear system can be ignored in conventional CMSRS method. An improved CMSRS method for considering the coupled damping, which is ignored in conventional CMSRS method, is proposed in this paper. Furthermore, a typical structure equipped with concentrated or coupled damper is taken as example to investigate the difference between the conventional and improved CMSRS methods.

2 Review of dynamic equations

The dynamic equations for a discrete, N-degree-of-freedom linear structural system subjected to M support motions can be written in following matrix form (Clough and Penzien 1993; Chopra 2001)

$$\begin{bmatrix} \boldsymbol{M} & \boldsymbol{M}_c \\ \boldsymbol{M}_c^T & \boldsymbol{M}_g \end{bmatrix} \begin{Bmatrix} \ddot{\boldsymbol{y}} \\ \ddot{\boldsymbol{u}}_g \end{Bmatrix} + \begin{bmatrix} \boldsymbol{C} & \boldsymbol{C}_c \\ \boldsymbol{C}_c^T & \boldsymbol{C}_g \end{bmatrix} \begin{Bmatrix} \dot{\boldsymbol{y}} \\ \dot{\boldsymbol{u}}_g \end{Bmatrix} + \begin{bmatrix} \boldsymbol{K} & \boldsymbol{K}_c \\ \boldsymbol{K}_c^T & \boldsymbol{K}_g \end{bmatrix} \begin{Bmatrix} \boldsymbol{y} \\ \boldsymbol{u}_g \end{Bmatrix} = \begin{Bmatrix} \vec{0} \\ \boldsymbol{P} \end{Bmatrix} \tag{1}$$

where $\boldsymbol{M}$, $\boldsymbol{C}$ and $\boldsymbol{K}$ are the $N \times N$ mass, damping and stiffness matrices associated with the unconstrained degrees of freedom, respectively; $\boldsymbol{M}_g$, $\boldsymbol{C}_g$ and $\boldsymbol{K}_g$ are the $M \times M$ mass, damping and stiffness matrices associated with the support degrees of freedom, and M is the numbers of constrained degrees of freedom; $\boldsymbol{M}_c$, $\boldsymbol{C}_c$ and $\boldsymbol{K}_c$ are $N \times M$ coupled mass, damping and stiffness matrices associated with both unconstrained and support degrees of freedom; symbol $\vec{0}$ denotes the n-dimensional zero vector; $\boldsymbol{P}$ is the m-vector of reacting forces at the support degrees of freedom; $\boldsymbol{y}$ is the total displacement vector at the unconstrained degrees of freedom, $\boldsymbol{u}_g$ is the m-vector of prescribed support displacements.

Expanding Eq. (1) gives

$$\boldsymbol{M}\ddot{\boldsymbol{y}} + \boldsymbol{M}_c\ddot{\boldsymbol{u}}_g + \boldsymbol{C}\dot{\boldsymbol{y}} + \boldsymbol{C}_c\dot{\boldsymbol{u}}_g + \boldsymbol{K}\boldsymbol{y} + \boldsymbol{K}_c\boldsymbol{u}_g = \vec{0} \tag{2}$$

It is common to decompose the response $\boldsymbol{y}$ into a pseudo-static component $\boldsymbol{y}^s$ and a dynamic component $\boldsymbol{y}^d$ as

$$\boldsymbol{y} = \boldsymbol{y}^s + \boldsymbol{y}^d \tag{3}$$

Substituting Eq. (3) into Eq. (2), the following equation can be obtained

$$\boldsymbol{M}\ddot{\boldsymbol{y}}^d + \boldsymbol{C}\dot{\boldsymbol{y}}^d + \boldsymbol{K}\boldsymbol{y}^d = -\left[\left(\boldsymbol{M}\ddot{\boldsymbol{y}}^s + \boldsymbol{M}_c\ddot{\boldsymbol{u}}_g\right) + \left(\boldsymbol{C}\dot{\boldsymbol{y}}^s + \boldsymbol{C}_c\dot{\boldsymbol{u}}_g\right) + \left(\boldsymbol{K}\boldsymbol{y}^s + \boldsymbol{K}_c\boldsymbol{u}_g\right)\right] \tag{4}$$

It is known that the third term on the right-hand of Eq. (4) remains zero. Therefore, the following relationship can be obtained

$$\boldsymbol{y}^s = -\boldsymbol{K}^{-1}\boldsymbol{K}_c\boldsymbol{u}_g = \boldsymbol{R}\boldsymbol{u}_g \tag{5}$$

where $\boldsymbol{R}$ denotes the influence matrix.

Substituting Eq. (5) into Eq. (4) yields

$$\boldsymbol{M}\ddot{\boldsymbol{y}}^d + \boldsymbol{C}\dot{\boldsymbol{y}}^d + \boldsymbol{K}\boldsymbol{y}^d = -(\boldsymbol{M}\boldsymbol{R} + \boldsymbol{M}_c)\ddot{\boldsymbol{u}}_g - (\boldsymbol{C}\boldsymbol{R} + \boldsymbol{C}_c)\dot{\boldsymbol{u}}_g \tag{6}$$

As the lumped mass model is adopted, the coupling mass matrix $\boldsymbol{M}_c$ remains zero. Equation (6) can be simplified as

$$\boldsymbol{M}\ddot{\boldsymbol{y}}^{d}+\boldsymbol{C}\dot{\boldsymbol{y}}^{d}+\boldsymbol{K}\boldsymbol{y}^{d}=-\boldsymbol{M}\boldsymbol{R}\ddot{\boldsymbol{u}}_{g}-(\boldsymbol{C}\boldsymbol{R}+\boldsymbol{C}_{c})\dot{\boldsymbol{u}}_{g} \tag{7}$$

It is debatable whether the term $\left((\boldsymbol{CR}+\boldsymbol{C}_{c})\dot{\boldsymbol{u}}_{g}\right)$ ignored by the conventional method is negligible in Eq. (7). In engineering practice, the supplemental damper of the structure has a significant influence on the coupled damping $\boldsymbol{C}_{c}$. Moreover, the value of the coupled damping increase with the increasing damping increment caused by the supplemental damper. Therefore, further study is given as follows.

3 Complex mode superposition method of seismic response for non-classically damped system

The free vibration equation for the classically damped linear system can be decoupled into classical modes due to the orthogonality of damping matrix (Caughey and O'kelly 1965). However, for the non-classically damped linear system, decoupling the vibration equation is difficult. Commonly, the matrix equations of the non-classically damped linear system are decoupled by the following approach (Foss 1958; Liang et al. 2012)

$$\boldsymbol{H}_{M}\dot{\boldsymbol{X}}+\boldsymbol{D}\boldsymbol{X}=-\boldsymbol{H}_{M}\boldsymbol{E}_{R}\ddot{\boldsymbol{u}}_{g}-(\boldsymbol{H}_{C}\boldsymbol{E}_{R}+\boldsymbol{H}_{C_{c}}\boldsymbol{E}_{I})\dot{\boldsymbol{u}}_{g} \tag{8}$$

where

$$\boldsymbol{H}_{M}=\begin{bmatrix}\boldsymbol{0} & \boldsymbol{M}\\ \boldsymbol{M} & \boldsymbol{C}\end{bmatrix} \tag{9-1}$$

$$\boldsymbol{H}_{C}=\begin{bmatrix}\boldsymbol{0} & \boldsymbol{C}\\ \boldsymbol{C} & \boldsymbol{C}\end{bmatrix} \tag{9-2}$$

$$\boldsymbol{H}_{C_{c}}=\begin{bmatrix}\boldsymbol{0} & \boldsymbol{C}_{c}^{T}\\ \boldsymbol{C}_{c} & \boldsymbol{C}\end{bmatrix} \tag{9-3}$$

$$\boldsymbol{D}=\begin{bmatrix}-\boldsymbol{M} & \boldsymbol{0}\\ \boldsymbol{0} & \boldsymbol{K}\end{bmatrix} \tag{9-4}$$

$$\boldsymbol{X}=\begin{pmatrix}\dot{\boldsymbol{y}}^{d}\\ \boldsymbol{y}^{d}\end{pmatrix} \tag{9-5}$$

$$\boldsymbol{E}_{R}=\begin{pmatrix}\boldsymbol{R}\\ \boldsymbol{0}\end{pmatrix} \tag{9-6}$$

$$\boldsymbol{E}_{I}=\begin{pmatrix}\boldsymbol{I}\\ \boldsymbol{0}\end{pmatrix} \tag{9-7}$$

where $\boldsymbol{I}$ and $\mathbf{0}$ denote the unit and zero matrices, respectively.

The solution of eigenproblem related to Eq. (8) can be transformed into the solution of the following equation

$$\boldsymbol{D}\boldsymbol{\Phi}=-\mu\boldsymbol{H}_{M}\boldsymbol{\Phi} \tag{10}$$

where μ and $\boldsymbol{\Phi}$ are eigenvalue and eigenvector, respectively.

According to Eq. (10), $\boldsymbol{\Phi}$ can be expressed as

$$\boldsymbol{\Phi}=(\mu\boldsymbol{\phi}\ \boldsymbol{\phi})^{T} \tag{11}$$

As the matrices $\boldsymbol{M}$, $\boldsymbol{C}$ and $\boldsymbol{K}$ are symmetric, the eigenvalues and eigenvectors deduced from Eq. (10) normally occur in complex conjugate pairs. Thus, ϕ and μ are given as

$$\boldsymbol{\phi} = \boldsymbol{\varphi} \pm i\boldsymbol{\psi} \tag{12}$$

$$\mu_j = -\xi_j\omega_j \pm i\omega_j\sqrt{1-\xi_j^2} \tag{13}$$

where ω_j and ξ_j represent the free vibration frequency and critical damping ratio of the j-th mode, respectively.

By substituting transformation

$$\boldsymbol{X} = \sum_{j=1}^{2N} \boldsymbol{\Phi}_j s_j(t) \tag{14}$$

into Eq. (8) and employing the generated orthogonal relation of eigenvectors, the decoupled dynamic equations are obtained as

$$\dot{s}_j(t) - \mu_j s_j(t) = -\sum_{k=1}^{M} \eta_{Mkj}\ddot{u}_{gk}(t) - \sum_{k=1}^{M} \eta_{Ckj}\dot{u}_{gk}(t) - \sum_{k=1}^{M} \eta_{C_ckj}\dot{u}_{gk}(t) \tag{15}$$

where $s_j(t)$ is the displacement response of the j-th single-degree-of-freedom (SDOF) oscillator with frequency ω_j and damping ratio ξ_j subjected to the given input force. The index k denotes the degree of freedom associated with the prescribed support motion, the subscript j denotes the mode number, and μ_j represents the structural complex eigenvalue, i.e.,

$$\mu_j = -\frac{(\boldsymbol{\Phi}_j)^T \boldsymbol{D}\boldsymbol{\Phi}_j}{(\boldsymbol{\Phi}_j)^T \boldsymbol{H}_M \boldsymbol{\Phi}_j} \tag{16}$$

and η_{Mkj}, η_{Ckj}, and η_{C_ckj} are the modal participation factors given by

$$\eta_{Mkj} = \frac{(\boldsymbol{\Phi}_j)^T \boldsymbol{H}_M \boldsymbol{E}_{Rk}}{\boldsymbol{L}_j} \tag{17}$$

$$\eta_{Ckj} = \frac{(\boldsymbol{\Phi}_j)^T \boldsymbol{H}_C \boldsymbol{E}_{Rk}}{\boldsymbol{L}_j} \tag{18}$$

$$\eta_{C_ckj} = \frac{(\boldsymbol{\Phi}_j)^T \boldsymbol{H}_{C_c} \boldsymbol{E}_{Ik}}{\boldsymbol{L}_j} \tag{19}$$

where $\boldsymbol{E}_{Rk}$ and $\boldsymbol{E}_{Ik}$ are the kth columns of the matrix $\boldsymbol{E}_R$ and $\boldsymbol{E}_I$ respectively and the denominator $\boldsymbol{L}_j$ is given by

$$\boldsymbol{L}_j = (\boldsymbol{\Phi}_j)^T \boldsymbol{H}_M \boldsymbol{\Phi}_j \tag{20}$$

Substituting Eqs. (9–1), (11), (12) d (13) into Eq. (20), $\boldsymbol{L}_j$ can be separated into real and imaginary parts as follows

$$\boldsymbol{L}_j = e_j + if_j \tag{21}$$

in which

$$e_j = -2\xi_j\omega_j\left(\left(\boldsymbol{\varphi}_j\right)^T\boldsymbol{M}\boldsymbol{\varphi}_j - \left(\boldsymbol{\psi}_j\right)^T\boldsymbol{M}\boldsymbol{\psi}_j\right) - 4\omega_j\sqrt{1-\xi_j^2}\left(\boldsymbol{\varphi}_j\right)^T\boldsymbol{M}\boldsymbol{\psi}_j + \left(\boldsymbol{\varphi}_j\right)^T\boldsymbol{C}\boldsymbol{\varphi}_j - \left(\boldsymbol{\psi}_j\right)^T\boldsymbol{C}\boldsymbol{\psi}_j \tag{22}$$

$$f_j = 2\omega_j\sqrt{1-\xi_j^2}\left(\left(\boldsymbol{\varphi}_j\right)^T\boldsymbol{M}\boldsymbol{\varphi}_j - \left(\boldsymbol{\psi}_j\right)^T\boldsymbol{M}\boldsymbol{\psi}_j\right) - 4\xi_j\omega_j\left(\boldsymbol{\varphi}_j\right)^T\boldsymbol{M}\boldsymbol{\psi}_j + 2\left(\boldsymbol{\varphi}_j\right)^T\boldsymbol{C}\boldsymbol{\psi}_j \tag{23}$$

Substituting Eqs. (21), (22) and (23) into Eq. (17) and separating the numerator of the right part of Eq. (17), η_{Mkj} can be expressed as

$$\eta_{Mkj} = \frac{1}{e_j^2+f_j^2}\left\{e_j\left(\boldsymbol{\varphi}_j\right)^T\boldsymbol{M}\boldsymbol{R}_k + f_j\left(\boldsymbol{\psi}_j\right)^T\boldsymbol{M}\boldsymbol{R}_k + i\left[e_j\left(\boldsymbol{\psi}_j\right)^T\boldsymbol{M}\boldsymbol{R}_k - f_j\left(\boldsymbol{\varphi}_j\right)^T\boldsymbol{M}\boldsymbol{R}_k\right]\right\} \tag{24}$$

The expressions of η_{Ckj} and η_{C_ckj} are obtained in a similar way

$$\eta_{Ckj} = \frac{1}{e_j^2+f_j^2}\left\{e_j\left(\boldsymbol{\varphi}_j\right)^T\boldsymbol{C}\boldsymbol{R}_k + f_j\left(\boldsymbol{\psi}_j\right)^T\boldsymbol{C}\boldsymbol{R}_k + i\left[e_j\left(\boldsymbol{\psi}_j\right)^T\boldsymbol{C}\boldsymbol{R}_k - f_j\left(\boldsymbol{\varphi}_j\right)^T\boldsymbol{C}\boldsymbol{R}_k\right]\right\} \tag{25}$$

$$\eta_{C_ckj} = \frac{1}{e_j^2+f_j^2}\left\{e_j\left(\boldsymbol{\varphi}_j\right)^T\boldsymbol{C}_c\boldsymbol{I}_k + f_j\left(\boldsymbol{\psi}_j\right)^T\boldsymbol{C}_c\boldsymbol{I}_k + i\left[e_j\left(\boldsymbol{\psi}_j\right)^T\boldsymbol{C}_c\boldsymbol{I}_k - f_j\left(\boldsymbol{\varphi}_j\right)^T\boldsymbol{C}_c\boldsymbol{I}_k\right]\right\} \tag{26}$$

It is convenient to define normazed responses $q_{\ddot{u}kj}(t)$ and $q_{\dot{u}kj}(t)$, representing the responses of SDOF oscillators with unit mass, frequency ω_j and damping ratio ξ_j, which are subjected to the base motions $\ddot{u}_k(t)$ and $\dot{u}_k(t)$, respectively.

Figure 1 shows the physical meaning of $q_{\ddot{u}ki}$. It is known that the structure responses of different modes under identical earthquake motion excitations are not the same. Moreover, the structure response varies with different ground motion excitation supports. Therefore, the SDOF oscillator is employed to represent each mode of the structure with acceleration excitation at different supports. Using modal analysis method, the dynamic component of response can be calculated by superposing the responses of each SDOF oscillator. The physical meaning of $q_{\dot{u}kj}(t)$ is almost the same as that of $q_{\ddot{u}kj}(t)$, and the only difference between them is that $q_{\dot{u}kj}(t)$ is generated under seismic velocity (instead of acceleration) excitation.

Substituting Eqs. (24), (25) and (26) into Eq. (15) and combining the terms consisted of a pair of conjugated complex modes, the following equation is obtained

$$\begin{aligned} y^d = &\sum_{k=1}^{M}\sum_{j=1}^{N}\left[\boldsymbol{A}_{Mkj}q_{\ddot{u}kj}(t) + \boldsymbol{B}_{Mkj}\dot{q}_{\ddot{u}kj}(t)\right] \\ &+ \sum_{k=1}^{M}\sum_{j=1}^{N}\left[\left(\boldsymbol{A}_{Ckj}+\boldsymbol{A}_{C_ckj}\right)q_{\dot{u}kj}(t) + \left(\boldsymbol{B}_{Ckj}+\boldsymbol{B}_{C_ckj}\right)\dot{q}_{\dot{u}kj}(t)\right] \end{aligned} \tag{27}$$

in which

$$\boldsymbol{A}_{Mkj} = \frac{2}{e_j^2+f_j^2}\left[\left(p_{Mkj}\xi_j + w_{Mkj}\sqrt{1-\xi_j^2}\right)\boldsymbol{\varphi}_j + \left(w_{Mkj}\xi_j - p_{Mkj}\sqrt{1-\xi_j^2}\right)\boldsymbol{\psi}_j\right]\omega_j \tag{28-1}$$

$$\boldsymbol{A}_{Ckj} = \frac{2}{e_j^2+f_j^2}\left[\left(p_{Ckj}\xi_j + w_{Ckj}\sqrt{1-\xi_j^2}\right)\boldsymbol{\varphi}_j + \left(w_{Ckj}\xi_j - p_{Ckj}\sqrt{1-\xi_j^2}\right)\boldsymbol{\psi}_j\right]\omega_j \tag{28-2}$$

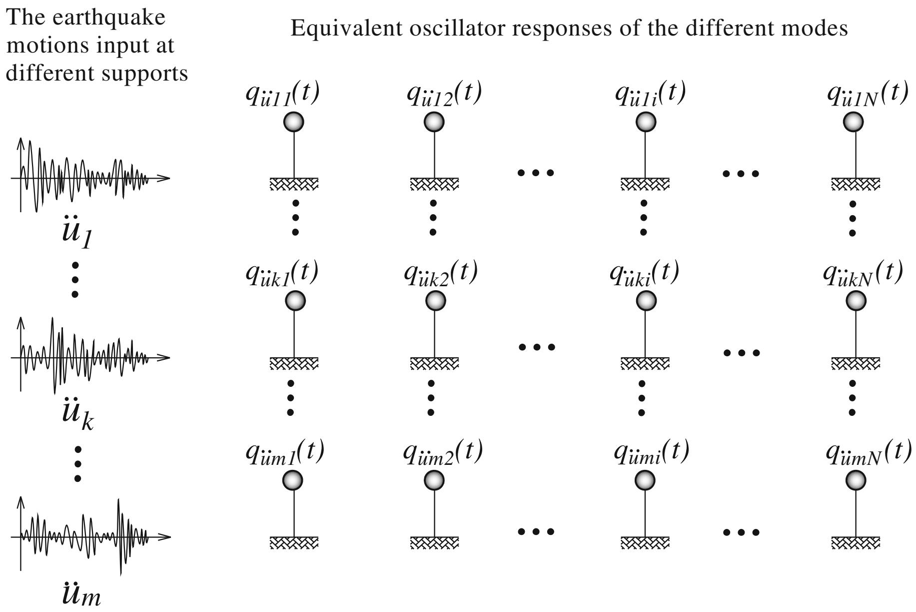

Fig. 1 Physical meanings for $q_{\ddot{u}ki}(k = 1 \sim M, i = 1 \sim N)$

$$\boldsymbol{A}_{C_c kj} = \frac{2}{e_j^2 + f_j^2}\left[\left(p_{C_c kj}\xi_j + w_{C_c kj}\sqrt{1-\xi_j^2}\right)\boldsymbol{\varphi}_j + \left(w_{C_c kj}\xi_j - p_{C_c kj}\sqrt{1-\xi_j^2}\right)\boldsymbol{\psi}_j\right]\omega_j \tag{28-3}$$

$$\boldsymbol{B}_{Mkj} = \frac{2}{e_j^2 + f_j^2}\left(p_{Mkj}\boldsymbol{\varphi}_j + w_{Mkj}\boldsymbol{\psi}_j\right) \tag{28-4}$$

$$\boldsymbol{B}_{Ckj} = \frac{2}{e_j^2 + f_j^2}\left(p_{Ckj}\boldsymbol{\varphi}_j + w_{Ckj}\boldsymbol{\psi}_j\right) \tag{28-5}$$

$$\boldsymbol{B}_{C_c kj} = \frac{2}{e_j^2 + f_j^2}\left(p_{C_c kj}\boldsymbol{\varphi}_j + w_{C_c kj}\boldsymbol{\psi}_j\right). \tag{28-6}$$

$$P_{Mkj} = e_j c_{Mkj} + f_j d_{Mkj}, \quad w_{Mkj} = f_j c_{Mkj} - e_j d_{Mkj} \tag{28-7}$$

$$P_{Ckj} = e_j c_{Ckj} + f_j d_{Ckj}, \quad w_{Ckj} = f_j c_{Ckj} - e_j d_{Ckj} \tag{28-8}$$

$$P_{C_c kj} = e_j c_{C_c kj} + f_j d_{C_c kj}, \quad w_{C_c kj} = f_j c_{C_c kj} - e_j d_{C_c kj} \tag{28-9}$$

$$c_{Mkj} = \left(\boldsymbol{\varphi}_j\right)^T \boldsymbol{M}\boldsymbol{R}_k, \quad d_{Mkj} = \left(\boldsymbol{\psi}_j\right)^T \boldsymbol{M}\boldsymbol{R}_k \tag{28-10}$$

$$c_{Ckj} = \left(\boldsymbol{\varphi}_j\right)^T \boldsymbol{C}\boldsymbol{R}_k, \quad d_{Ckj} = \left(\boldsymbol{\psi}_j\right)^T \boldsymbol{C}\boldsymbol{R}_k \tag{28-11}$$

$$c_{Ckj} = \left(\boldsymbol{\varphi}_j\right)^T \boldsymbol{C}_c\boldsymbol{I}_k, \quad d_{C_c kj} = \left(\boldsymbol{\psi}_j\right)^T \boldsymbol{C}_c\boldsymbol{I}_k \tag{28-12}$$

As mentioned above, the two terms, $q_{\ddot{u}kj}(t)$ and $q_{\dot{u}kj}(t)$, can be expressed as the solutions of Eqs. (29-1) and (29-2), respectively:

$$\ddot{q}_{\ddot{u}j}(t) + 2\xi_j\omega_j\dot{q}_{\ddot{u}j}(t) + \omega_j^2 q_{\ddot{u}j}(t) = -\ddot{u}_{gk}(t) \tag{29-1}$$

$$\ddot{q}_{\dot{u}j}(t) + 2\xi_j\omega_j\dot{q}_{\dot{u}j}(t) + \omega_j^2 q_{\dot{u}j}(t) = -\dot{u}_{gk}(t) \tag{29-2}$$

A generic response quantity or effect of interest, $z(t)$ (e.g., a nodal displacement, an internal force, stress or strain component), can be expressed as a linear function of the nodal displacements $\boldsymbol{y}(t)$, i.e.,

$$z(t) = \boldsymbol{v}^T\boldsymbol{y}(t) = \boldsymbol{v}^T\left[\boldsymbol{y}^s(t) + \boldsymbol{y}^d(t)\right] \tag{30}$$

where $\boldsymbol{v}$ is a response transfer vector which usually depends on the geometry and stiffness properties of the structure. Substituting Eqs. (5) and (27) into Eq. (30), the generic response $z(t)$ is written as

$$\begin{aligned} z(t) = {} & \sum_{k=1}^{M}\boldsymbol{g}_k u_k(t) + \sum_{k=1}^{M}\sum_{j=1}^{N}\left[\boldsymbol{a}_{Mkj}q_{\ddot{u}kj}(t) + \boldsymbol{b}_{Mkj}\dot{q}_{\ddot{u}j}(t)\right] \\ & + \sum_{k=1}^{M}\sum_{j=1}^{N}\left[\left(\boldsymbol{a}_{Ckj} + \boldsymbol{a}_{C_ckj}\right)q_{\dot{u}kj}(t) + \left(\boldsymbol{b}_{Ckj} + \boldsymbol{b}_{C_ckj}\right)q_{\dot{u}kj}(t)\right] \end{aligned} \tag{31}$$

in which

$$\boldsymbol{g}_k = v^T\boldsymbol{R}_k \tag{32-1}$$

$$\boldsymbol{a}_{Mkj} = v^T\boldsymbol{A}_{Mkj}, \quad \boldsymbol{b}_{Mkj} = v^T\boldsymbol{B}_{Mkj} \tag{32-2}$$

$$\boldsymbol{a}_{Ckj} = v^T\boldsymbol{A}_{Ckj}, \quad \boldsymbol{b}_{Ckj} = v^T\boldsymbol{B}_{Ckj} \tag{32-3}$$

$$\boldsymbol{a}_{C_ckj} = v^T\boldsymbol{A}_{C_ckj}, \quad \boldsymbol{b}_{C_ckj} = v^T\boldsymbol{B}_{C_ckj} \tag{32-4}$$

where $\boldsymbol{g}_k$ denotes the effective influence coefficients; $\boldsymbol{a}_{Mkj}$, $\boldsymbol{b}_{Mkj}$, $\boldsymbol{a}_{Ckj}$, $\boldsymbol{b}_{Ckj}$, $\boldsymbol{a}_{C_ckj}$ and $\boldsymbol{b}_{C_ckj}$ represent the effective modal participation factors. The first sum on the right-hand side of Eq. (31) represents the pseudo-static component of the response and the other two terms on the right side represent the dynamic components. It should be noted that $\boldsymbol{g}_k$, $\boldsymbol{a}_{Mkj}$, $\boldsymbol{b}_{Mkj}$, $\boldsymbol{a}_{Ckj}$, $\boldsymbol{b}_{Ckj}$, $\boldsymbol{a}_{C_ckj}$ and $\boldsymbol{b}_{C_ckj}$ are mainly dependent on the structural properties, i.e., mass, stiffness, damping ratio, eigenvalues and eigenvectors.

4 Mean-square stationary response of the system under random disturbance

In this section, the response spectrum formula is developed based on the random vibration theory. Firstly, the support motions $\ddot{u}_{gk}$ and $\dot{u}_{gk}$ are regarded as jointly stationary processes with zero means. Thus, the response of each mode of the structure is also stationary. These assumptions are reasonable for the intended purpose as long as the fundamental period of structural vibration is relatively short compared with the duration of excitation. Based on Eq. (31), the power spectral density of the generic steady state response z (t) can be written as

$$
\begin{aligned}
G_{zz}(t) =& \sum_{k=1}^{M}\sum_{l=1}^{M} \boldsymbol{g}_k \boldsymbol{g}_l G_{u_k u_l}(i\omega) + 2\sum_{k=1}^{M}\sum_{l=1}^{M}\sum_{j=1}^{N} \left(\boldsymbol{g}_k \boldsymbol{a}_{Mlj} + i\omega \boldsymbol{g}_k \boldsymbol{b}_{Mlj}\right) H_j(-i\omega) G_{u_k \ddot{u}_l}(i\omega) \\
&+ 2\sum_{k=1}^{M}\sum_{l=1}^{M}\sum_{j=1}^{N} \left[\boldsymbol{g}_k \left(\boldsymbol{a}_{Clj} + \boldsymbol{a}_{C_c lj}\right) + i\omega \boldsymbol{g}_k \left(\boldsymbol{b}_{Clj} + \boldsymbol{b}_{C_c lj}\right)\right] H_j(-i\omega) G_{u_k \dot{u}_l}(i\omega) \\
&+ \sum_{k=1}^{M}\sum_{l=1}^{M}\sum_{i=1}^{N}\sum_{j=1}^{N} \left(\boldsymbol{a}_{Mki}\boldsymbol{a}_{Mlj} + 2i\omega \boldsymbol{b}_{Mki}\boldsymbol{a}_{Mlj} + \omega^2 \boldsymbol{g}_k \boldsymbol{b}_{Mki}\boldsymbol{b}_{Mlj}\right) H_i(i\omega) H_j(-i\omega) G_{\ddot{u}_k \ddot{u}_l}(i\omega) \\
&+ 2\sum_{k=1}^{M}\sum_{l=1}^{M}\sum_{i=1}^{N}\sum_{j=1}^{N} \left[\boldsymbol{a}_{Mki}\left(\boldsymbol{a}_{Clj} + \boldsymbol{a}_{C_c lj}\right) + i\omega \boldsymbol{a}_{Mki}\left(\boldsymbol{b}_{Clj} + \boldsymbol{b}_{C_c lj}\right) + i\omega \boldsymbol{b}_{Mki}\left(\boldsymbol{a}_{Clj} + \boldsymbol{a}_{C_c lj}\right)\right. \\
&\left. + \omega^2 \boldsymbol{b}_{Mki}\left(\boldsymbol{b}_{Clj} + \boldsymbol{b}_{C_c lj}\right)\right] H_i(i\omega) H_j(-i\omega) G_{\ddot{u}_k \dot{u}_l}(i\omega) \\
&+ \sum_{k=1}^{M}\sum_{l=1}^{M}\sum_{i=1}^{N}\sum_{j=1}^{N} \left[\left(\boldsymbol{a}_{Cki} + \boldsymbol{a}_{C_c ki}\right)\left(\boldsymbol{a}_{Clj} + \boldsymbol{a}_{C_c lj}\right) + 2i\omega \boldsymbol{a}_{Mki}\left(\boldsymbol{a}_{Cki} + \boldsymbol{a}_{C_c ki}\right)\left(\boldsymbol{b}_{Clj} + \boldsymbol{b}_{C_c lj}\right)\right. \\
&\left. + \omega^2 \left(\boldsymbol{b}_{Cki} + \boldsymbol{b}_{C_c ki}\right)\left(\boldsymbol{b}_{Clj} + \boldsymbol{b}_{C_c lj}\right)\right] H_i(i\omega) H_j(-i\omega) G_{\dot{u}_k \dot{u}_l}(i\omega)
\end{aligned} \tag{33}
$$

in which $G_{xy}(i\omega)$. represents the cross-power spectral density of process x and y, and $H_i(i\omega)$ is given as

$$
H_i(i\omega) = H_j\left(\omega_i^2 - \omega^2 + 2i\xi_i\omega_i\omega\right)^{-1} \tag{34}
$$

where $H_i(i\omega)$ denotes the frequency response function of i-th mode.

For Eq. (33), integrating over the frequency domain $-\infty < \omega < \infty$, the mean-square response yields

$$
\begin{aligned}
\sigma_z^2 =& \sum_{k=1}^{M}\sum_{l=1}^{M} \boldsymbol{g}_k \boldsymbol{g}_l \rho_{u_k u_l}\sigma_{u_k}\sigma_{u_l} + 2\sum_{k=1}^{M}\sum_{l=1}^{M}\sum_{j=1}^{N}\left(\boldsymbol{g}_k \boldsymbol{a}_{Mlj}\rho_{u_k q_{\ddot{u}lj}}\sigma_{u_k}\sigma_{q_{\ddot{u}lj}} + \boldsymbol{g}_k \boldsymbol{b}_{Mlj}\rho_{u_k \dot{q}_{\ddot{u}lj}}\sigma_{u_k}\sigma_{\dot{q}_{\ddot{u}lj}}\right) \\
&+ 2\sum_{k=1}^{M}\sum_{l=1}^{M}\sum_{j=1}^{N}\left[\boldsymbol{g}_k\left(\boldsymbol{a}_{Clj} + \boldsymbol{a}_{C_c lj}\right)\rho_{u_k q_{\dot{u}lj}}\sigma_{u_k}\sigma_{q_{\dot{u}lj}} + i\omega \boldsymbol{g}_k\left(\boldsymbol{b}_{Clj} + \boldsymbol{b}_{C_c lj}\right)\rho_{u_k \dot{q}_{\dot{u}lj}}\sigma_{u_k}\sigma_{\dot{q}_{\dot{u}lj}}\right] \\
&+ \sum_{k=1}^{M}\sum_{l=1}^{M}\sum_{i=1}^{N}\sum_{j=1}^{N}\left(\boldsymbol{a}_{Mki}\boldsymbol{a}_{Mlj}\rho_{q_{\ddot{u}ki}q_{\ddot{u}lj}}\sigma_{q_{\ddot{u}ki}}\sigma_{q_{\ddot{u}lj}} + 2\boldsymbol{b}_{Mki}\boldsymbol{a}_{Mlj}\rho_{\dot{q}_{\ddot{u}ki}q_{\ddot{u}lj}}\sigma_{\dot{q}_{\ddot{u}ki}}\sigma_{q_{\ddot{u}lj}}\right. \\
&\left. + \boldsymbol{b}_{Mki}\boldsymbol{b}_{Mlj}\rho_{\dot{q}_{\ddot{u}ki}\dot{q}_{\ddot{u}lj}}\sigma_{\dot{q}_{\ddot{u}ki}}\sigma_{\dot{q}_{\ddot{u}lj}}\right) \\
&+ 2\sum_{k=1}^{M}\sum_{l=1}^{M}\sum_{i=1}^{N}\sum_{j=1}^{N}\left[\boldsymbol{a}_{Mki}\left(\boldsymbol{a}_{Clj} + \boldsymbol{a}_{C_c lj}\right)\rho_{q_{\ddot{u}ki}q_{\dot{u}kj}}\sigma_{q_{\ddot{u}ki}}\sigma_{q_{\dot{u}kj}} + \boldsymbol{a}_{Mki}\left(\boldsymbol{b}_{Clj} + \boldsymbol{b}_{C_c lj}\right)\rho_{q_{\ddot{u}ki}\dot{q}_{\dot{u}lj}}\sigma_{q_{\ddot{u}ki}}\sigma_{\dot{q}_{\dot{u}lj}}\right. \\
&\left. + \boldsymbol{b}_{Mki}\left(\boldsymbol{a}_{Clj} + \boldsymbol{a}_{C_c lj}\right)\rho_{\dot{q}_{\ddot{u}ki}q_{\dot{u}lj}}\sigma_{\dot{q}_{\ddot{u}ki}}\sigma_{q_{\dot{u}lj}} + \boldsymbol{b}_{Mki}\left(\boldsymbol{b}_{Clj} + \boldsymbol{b}_{C_c lj}\right)\rho_{\dot{q}_{\ddot{u}ki}\dot{q}_{\dot{u}lj}}\sigma_{\dot{q}_{\ddot{u}ki}}\sigma_{\dot{q}_{\dot{u}lj}}\right] \\
&+ \sum_{k=1}^{M}\sum_{l=1}^{M}\sum_{i=1}^{N}\sum_{j=1}^{N}\left[\left(\boldsymbol{a}_{Cki} + \boldsymbol{a}_{C_c ki}\right)\left(\boldsymbol{a}_{Clj} + \boldsymbol{a}_{C_c lj}\right)\rho_{q_{\dot{u}ki}q_{\dot{u}lj}}\sigma_{q_{\dot{u}ki}}\sigma_{q_{\dot{u}lj}}\right. \\
&\left. + 2\left(\boldsymbol{a}_{Cki} + \boldsymbol{a}_{C_c ki}\right)\left(\boldsymbol{b}_{Clj} + \boldsymbol{b}_{C_c lj}\right)\rho_{q_{\dot{u}ki}\dot{q}_{\dot{u}lj}}\sigma_{q_{\dot{u}ki}}\sigma_{\dot{q}_{\dot{u}lj}} + \left(\boldsymbol{b}_{Cki} + \boldsymbol{b}_{C_c ki}\right)\left(\boldsymbol{b}_{Clj} + \boldsymbol{b}_{C_c lj}\right)\rho_{\dot{q}_{\dot{u}ki}\dot{q}_{\dot{u}lj}}\sigma_{\dot{q}_{\dot{u}ki}}\sigma_{\dot{q}_{\dot{u}lj}}\right]
\end{aligned} \tag{35}
$$

in which σ_{u_k}, $\sigma_{q_{ki}}$ and $\sigma_{\dot{q}_{ki}}$ are the mean-square-root of the ground displacement $u_k(t)$, normalized modal displacement response q_{ki} and the normalized modal velocity response

$\dot{q}_{ki}$; $\rho_{u_k u_l}$, $\rho_{u_k q_{\ddot{u}lj}}$, $\rho_{u_k \dot{q}_{\ddot{u}lj}}$, $\rho_{u_k q_{\dot{u}kj}}$, $\rho_{u_k \dot{q}_{\dot{u}kj}}$, $\rho_{q_{\ddot{u}ki} q_{\ddot{u}lj}}$, $\rho_{\dot{q}_{\ddot{u}ki} q_{\ddot{u}lj}}$, $\rho_{\dot{q}_{\ddot{u}ki} \dot{q}_{\ddot{u}lj}}$, $\rho_{q_{\ddot{u}ki} q_{\dot{u}kj}}$, $\rho_{q_{\ddot{u}ki} \dot{q}_{\dot{u}lj}}$, $\rho_{\dot{q}_{\ddot{u}ki} q_{\dot{u}lj}}$, $\rho_{\dot{q}_{\ddot{u}ki} \dot{q}_{\dot{u}lj}}$, $\rho_{q_{\dot{u}ki} q_{\dot{u}lj}}$, $\rho_{q_{\dot{u}ki} \dot{q}_{\dot{u}lj}}$, and $\rho_{\dot{q}_{\dot{u}ki} \dot{q}_{\dot{u}lj}}$ are the corresponding cross-correlation coefficients; $\sigma_{\dot{q}_{\ddot{u}ki}}$ and $\sigma_{\dot{q}_{\dot{u}ki}}$ represent the mean-square-root of velocity response $\dot{q}_{ki}$ subjected to support acceleration motion $\ddot{u}_k$ and support velocity motion $\dot{u}_k$ respectively, and the expressions of $\sigma_{\dot{q}_{\ddot{u}ki}}$ and $\sigma_{\dot{q}_{\dot{u}ki}}$ are given as follows

$$\sigma^2_{\dot{q}_{\ddot{u}ki}} = \int_{-\infty}^{\infty} \omega^2 |H_i(i\omega)|^2 G_{\ddot{u}_k \ddot{u}_k}(\omega) d\omega \tag{36}$$

$$\sigma^2_{\dot{q}_{\dot{u}ki}} = \int_{-\infty}^{\infty} \omega^2 |H_i(i\omega)|^2 G_{\dot{u}_k \dot{u}_k}(\omega) d\omega \tag{37}$$

where $G_{\ddot{u}_k \ddot{u}_k}(\omega)$ and $G_{\dot{u}_k \dot{u}_k}(\omega)$ are the real-valued power spectral densities of input acceleration and velocity. Furthermore, the cross-correlation coefficients mentioned in Eq. (35) can be defined as follows

$$\rho_{u_k u_l} = \frac{1}{\sigma_{u_k} \sigma_{u_l}} \int_{-\infty}^{\infty} G_{u_k u_l}(i\omega) d\omega \tag{38-1}$$

$$\rho_{u_k q_{\ddot{u}lj}} = \frac{1}{\sigma_{u_k} \sigma_{q_{\ddot{u}lj}}} \int_{-\infty}^{\infty} H_j(-i\omega) G_{u_k \ddot{u}_l}(i\omega) d\omega \tag{38-2}$$

$$\rho_{u_k \dot{q}_{\ddot{u}lj}} = \frac{1}{\sigma_{u_k} \sigma_{\dot{q}_{\ddot{u}lj}}} \int_{-\infty}^{\infty} i\omega H_j(-i\omega) G_{u_k \ddot{u}_l}(i\omega) d\omega \tag{38-3}$$

$$\rho_{u_k q_{\dot{u}lj}} = \frac{1}{\sigma_{u_k} \sigma_{q_{\dot{u}lj}}} \int_{-\infty}^{\infty} H_j(-i\omega) G_{u_k \dot{u}_l}(i\omega) d\omega \tag{38-4}$$

$$\rho_{u_k \dot{q}_{\dot{u}lj}} = \frac{1}{\sigma_{u_k} \sigma_{\dot{q}_{\dot{u}lj}}} \int_{-\infty}^{\infty} i\omega H_j(-i\omega) G_{u_k \dot{u}_l}(i\omega) d\omega \tag{38-5}$$

$$\rho_{q_{\ddot{u}ki} q_{\ddot{u}lj}} = \frac{1}{\sigma_{q_{\ddot{u}ki}} \sigma_{q_{\ddot{u}lj}}} \int_{-\infty}^{\infty} H_i(i\omega) H_j(-i\omega) G_{\ddot{u}_k \ddot{u}_l}(i\omega) d\omega \tag{38-6}$$

$$\rho_{\dot{q}_{\ddot{u}ki} q_{\ddot{u}lj}} = \frac{1}{\sigma_{\dot{q}_{\ddot{u}ki}} \sigma_{q_{\ddot{u}lj}}} \int_{-\infty}^{\infty} i\omega H_i(i\omega) H_j(-i\omega) G_{\ddot{u}_k \ddot{u}_l}(i\omega) d\omega \tag{38-7}$$

$$\rho_{\dot{q}_{\ddot{u}ki} \dot{q}_{\ddot{u}lj}} = \frac{1}{\sigma_{\dot{q}_{\ddot{u}ki}} \sigma_{\dot{q}_{\ddot{u}lj}}} \int_{-\infty}^{\infty} \omega^2 H_i(i\omega) H_j(-i\omega) G_{\ddot{u}_k \ddot{u}_l}(i\omega) d\omega \tag{38-8}$$

$$\rho_{q_{\ddot{u}ki}q_{\dot{u}lj}} = \frac{1}{\sigma_{q_{\ddot{u}ki}}\sigma_{q_{\dot{u}lj}}} \int_{-\infty}^{\infty} H_i(i\omega)H_j(-i\omega)G_{\ddot{u}_k\dot{u}_l}(i\omega)d\omega \tag{38-9}$$

$$\rho_{q_{\ddot{u}ki}\dot{q}_{\dot{u}lj}} = \frac{1}{\sigma_{q_{\ddot{u}ki}}\sigma_{\dot{q}_{\dot{u}kj}}} \int_{-\infty}^{\infty} H_i(i\omega)H_j(-i\omega)G_{\ddot{u}_k\dot{u}_l}(i\omega)d\omega \tag{38-10}$$

$$\rho_{\dot{q}_{\ddot{u}ki}q_{\dot{u}lj}} = \frac{1}{\sigma_{\dot{q}_{\ddot{u}ki}}\sigma_{q_{\dot{u}lj}}} \int_{-\infty}^{\infty} i\omega H_i(i\omega)H_j(-i\omega)G_{\ddot{u}_k\dot{u}_l}(i\omega)d\omega \tag{38-11}$$

$$\rho_{\dot{q}_{\ddot{u}ki}\dot{q}_{\dot{u}lj}} = \frac{1}{\sigma_{\dot{q}_{\ddot{u}ki}}\sigma_{\dot{q}_{\dot{u}lj}}} \int_{-\infty}^{\infty} \omega^2 H_i(i\omega)H_j(-i\omega)G_{\ddot{u}_k\dot{u}_l}(i\omega)d\omega \tag{38-12}$$

$$\rho_{q_{\dot{u}ki}q_{\dot{u}lj}} = \frac{1}{\sigma_{q_{\dot{u}ki}}\sigma_{q_{\dot{u}lj}}} \int_{-\infty}^{\infty} H_i(i\omega)H_j(-i\omega)G_{\dot{u}_k\dot{u}_l}(i\omega)d\omega \tag{38-13}$$

$$\rho_{q_{\dot{u}ki}\dot{q}_{\dot{u}lj}} = \frac{1}{\sigma_{q_{\dot{u}ki}}\sigma_{\dot{q}_{\dot{u}lj}}} \int_{-\infty}^{\infty} i\omega H_i(i\omega)H_j(-i\omega)G_{\dot{u}_k\dot{u}_l}(i\omega)d\omega \tag{38-14}$$

$$\rho_{\dot{q}_{\dot{u}ki}\dot{q}_{\dot{u}lj}} = \frac{1}{\sigma_{\dot{q}_{\dot{u}ki}}\sigma_{\dot{q}_{\dot{u}lj}}} \int_{-\infty}^{\infty} \omega^2 H_i(i\omega)H_j(-i\omega)G_{\dot{u}_k\dot{u}_l}(i\omega)d\omega \tag{38-15}$$

Each of the above integrands has an anti-symmetric imaginary part. Hence, their integrals have real values. The nine cross-correlation coefficients, i.e., $\rho_{u_k q_{\dot{u}lj}}$, $\rho_{u_k \dot{q}_{\dot{u}lj}}$, $\rho_{q_{\ddot{u}ki}q_{\dot{u}lj}}$, $\rho_{q_{\ddot{u}ki}\dot{q}_{\dot{u}lj}}$, $\rho_{\dot{q}_{\ddot{u}ki}q_{\dot{u}lj}}$, $\rho_{\dot{q}_{\ddot{u}ki}\dot{q}_{\dot{u}lj}}$, $\rho_{q_{\dot{u}ki}q_{\dot{u}lj}}$, $\rho_{q_{\dot{u}ki}\dot{q}_{\dot{u}lj}}$, and $\rho_{\dot{q}_{\dot{u}ki}\dot{q}_{\dot{u}lj}}$ are introduced for the first time to the authors' knowledge.

The cross-correlation coefficies in Eqs. (38-1) to (38-6) have been discussed by Kiureghian and Neumnhofer (1992) and Yu and Zhou (2008), and the other cross-correlation coefficients are interpreted as follows. Specifically, $\rho_{u_k q_{\dot{u}lj}}$ des the cross-correlation coefficient between the forced displacement at support k and the modal displacement response of the oscillator subjected to support velocity $\dot{u}_k$ corresponding to mode j; $\rho_{u_k \dot{q}_{\dot{u}lj}}$ denotes the cross-correlation coefficient between the forced displacement at support k and the modal velocity response of the oscillator subjected to support velocity $\dot{u}_k$ corresponding to mode j. As shown in Eqs. (38-8)–(38-15), these eight cross-correlation coefficients can be expressed in terms of a pair of oscillators representing modes i and j of the structure. Table 1 shows the physical meanings of the cross-correlation coefficients in (38-8)–(38-15).

Based on above discussions, the improved complex multiple-support response spectrum method for non-classically damped linear system is deduced on the basis of previous works (Kiureghian and Neumnhofer 1992; Zerva 1990; Yu and Zhou 2008). Assuming that the root-mean-squares of the ground displacement, oscillator displacement response and velocity response corresponding to different modes and support motion inputs, i.e., σ_{u_k}, $\sigma_{q_{\dot{u}ki}}$, $\sigma_{\dot{q}_{\dot{u}ki}}$, $\sigma_{q_{\ddot{u}lj}}$ and $\sigma_{\dot{q}_{\ddot{u}ki}}$ are proportional to the peak values of the seismic response (Kiureghian and Neumnhofer 1992), the following formula can be obtained.

Table 1 The physical meanings of each cross-correlation coefficient in Eqs. (38-8) to (38-15)

Cross-correlation coefficient	Oscillator 1				Oscillator 2			
	Support motion input	Support degree-of-freedom	Response type	Mode	Support motion input	Support degree-of-freedom	Response type	Mode
$\rho_{q_{\ddot{u}ki}q_{\dot{u}lj}}$	Acceleration	k	Displacement	i	Velocity	l	Displacement	j
$\rho_{q_{\ddot{u}ki}\dot{q}_{\ddot{u}lj}}$	Acceleration	k	Displacement	i	Acceleration	l	Velocity	j
$\rho_{\dot{q}_{\ddot{u}ki}q_{\dot{u}lj}}$	Acceleration	k	Velocity	i	Velocity	l	Displacement	j
$\rho_{\dot{q}_{\ddot{u}ki}\dot{q}_{\dot{u}lj}}$	Acceleration	k	Velocity	i	Velocity	l	Velocity	j
$\rho_{q_{\dot{u}ki}q_{\dot{u}lj}}$	Velocity	k	Displacement	i	Velocity	l	Displacement	j
$\rho_{q_{\dot{u}ki}\dot{q}_{\dot{u}lj}}$	Velocity	k	Displacement	i	Velocity	l	Velocity	j
$\rho_{\dot{q}_{\dot{u}ki}\dot{q}_{\dot{u}lj}}$	Velocity	k	Velocity	i	Velocity	l	Velocity	j

$$
\begin{aligned}
|z(t)|_{max}=\Bigg\{&\sum_{k=1}^{M}\sum_{l=1}^{M}\boldsymbol{g}_k\boldsymbol{g}_l\rho_{u_k u_l}u_{k,max}u_{l,max}\\
&+2\sum_{k=1}^{M}\sum_{l=1}^{M}\sum_{j=1}^{N}\Big[\Big(\boldsymbol{g}_k\boldsymbol{a}_{Mlj}\rho_{u_k q_{\ddot{u}lj}}+\boldsymbol{g}_k\boldsymbol{b}_{Mlj}\omega_j\rho_{u_k\dot{q}_{\ddot{u}lj}}\Big)u_{k,max}D_{\ddot{u}l}\big(\omega_j,\xi_j\big)\Big]\\
&+2\sum_{k=1}^{M}\sum_{l=1}^{M}\sum_{j=1}^{N}\Big[\boldsymbol{g}_k\big(\boldsymbol{a}_{Clj}+\boldsymbol{a}_{C_c lj}\big)\rho_{u_k q_{\dot{u}kj}}+\boldsymbol{g}_k\big(\boldsymbol{b}_{Clj}+\boldsymbol{b}_{C_c lj}\big)\rho_{u_k\dot{q}_{\dot{u}kj}}\Big]u_{k,max}D_{\dot{u}l}\big(\omega_j,\xi_j\big)\\
&+\sum_{k=1}^{M}\sum_{l=1}^{M}\sum_{i=1}^{N}\sum_{j=1}^{N}\Big[\big(\boldsymbol{a}_{Mki}\boldsymbol{a}_{Mlj}\rho_{q_{\ddot{u}ki}q_{\ddot{u}lj}}+2\boldsymbol{b}_{Mki}a_{Mlj}\rho_{\dot{q}_{\ddot{u}ki}q_{\ddot{u}lj}}\sigma_{\dot{q}_{\ddot{u}ki}}\sigma_{q_{\ddot{u}lj}}\\
&+\boldsymbol{b}_{Mki}\boldsymbol{b}_{Mlj}\omega_i\omega_j\rho_{\dot{q}_{\ddot{u}ki}\dot{q}_{\ddot{u}lj}}\big)D_{\ddot{u}k}(\omega_i,\xi_i)D_{\ddot{u}l}\big(\omega_j,\xi_j\big)\Big]\\
&+2\sum_{k=1}^{M}\sum_{l=1}^{M}\sum_{i=1}^{N}\sum_{j=1}^{N}\Big\{\big[\boldsymbol{a}_{Mki}\big(\boldsymbol{a}_{Clj}+\boldsymbol{a}_{C_c lj}\big)\rho_{q_{\ddot{u}ki}q_{\dot{u}kj}}+\boldsymbol{a}_{Mki}\big(\boldsymbol{b}_{Clj}+\boldsymbol{b}_{C_c lj}\big)\rho_{q_{\ddot{u}ki}\dot{q}_{\dot{u}lj}}\\
&+\boldsymbol{b}_{Mki}\big(\boldsymbol{a}_{Clj}+\boldsymbol{a}_{C_c lj}\big)\omega_i\rho_{\dot{q}_{\ddot{u}ki}q_{\dot{u}lj}}+\boldsymbol{b}_{Mki}\big(\boldsymbol{b}_{Clj}+\boldsymbol{b}_{C_c lj}\big)\omega_i\omega_j\rho_{\dot{q}_{\ddot{u}ki}\dot{q}_{\dot{u}lj}}\big]D_{\ddot{u}k}(\omega_i,\xi_i)D_{\dot{u}l}\big(\omega_j,\xi_j\big)\Big\}\\
&+\sum_{k=1}^{M}\sum_{l=1}^{M}\sum_{i=1}^{N}\sum_{j=1}^{N}\Big[\big(\boldsymbol{a}_{Cki}+\boldsymbol{a}_{C_c ki}\big)\big(\boldsymbol{a}_{Clj}+\boldsymbol{a}_{C_c lj}\big)\rho_{q_{\dot{u}ki}q_{\dot{u}lj}}\\
&+2\big(\boldsymbol{a}_{Cki}+\boldsymbol{a}_{C_c ki}\big)\big(\boldsymbol{b}_{Clj}+\boldsymbol{b}_{C_c lj}\big)\omega_j\rho_{q_{\dot{u}ki}\dot{q}_{\dot{u}lj}}\\
&+\big(\boldsymbol{b}_{Cki}+\boldsymbol{b}_{C_c ki}\big)\big(\boldsymbol{b}_{Clj}+\boldsymbol{b}_{C_c lj}\big)\omega_i\omega_j\rho_{\dot{q}_{\dot{u}ki}\dot{q}_{\dot{u}lj}}\Big]D_{\dot{u}k}(\omega_i,\xi_i)D_{\dot{u}l}\big(\omega_j,\xi_j\big)\Bigg\}^{1/2}
\end{aligned}
\tag{39}
$$

in which

$$u_{k,max} = E[max|u_k(t)|] \tag{40-1}$$

$$u_{l,max} = E[max|u_l(t)|] \tag{40-2}$$

$$D_{\ddot{u}k}(\omega_i, \xi_i) = E[max|q_{\ddot{u}ki}(t)|] \tag{40-3}$$

$$D_{\ddot{u}l}\big(\omega_j, \xi_j\big) = E\big[max\big|q_{\ddot{u}lj}(t)\big|\big] \tag{40-4}$$

$$D_{\dot{u}k}(\omega_i, \xi_i) = E[max|q_{\dot{u}ki}(t)|] \tag{40-5}$$

$$D_{\dot{u}l}\big(\omega_j, \xi_j\big) = E\big[max\big|q_{\dot{u}lj}(t)\big|\big] \tag{40-6}$$

where $u_{k,max}$ and $u_{l,max}$ denote the mean value of the peak displacements at support k and l, respectively; $D_{\ddot{u}k}(\omega_i, \xi_i)$ denotes the mean response spectrum ordinate for the oscillator of i-th mode subjected to the support motion $\ddot{u}_k$; $D_{\ddot{u}l}\big(\omega_j, \xi_j\big)$ denotes the mean response spectrum ordinate for the oscillator of j-th mode subjected to the support motion $\ddot{u}_l$; $D_{\dot{u}k}(\omega_i, \xi_i)$ denotes the mean response spectrum ordinate for the oscillator of i-th mode subjected to the support motion $\dot{u}_k$; $D_{\dot{u}l}\big(\omega_j, \xi_j\big)$ denotes the mean response spectrum ordinate for the oscillator of j-th mode subjected to the support motion $\dot{u}_l$. It is noted that for the structure equipped with supplemental dampers, some over damped modes may be present and in such a case the proposed approach is inapplicable.

It should be noted that the time history analysis is included in the proposed frequency-domain method (Eq. (40)). The first two parameters $u_{k,max}$ and $u_{l,max}$ in Eq. (40) can be easily determined according to the seismic design codes. However, the other parameters have to be calculated through the time history analysis for the SDOF system, which makes the advantage of the response spectrum method partly lost. For the structural dynamic analysis considering multi-support seismic excitations, the time-domain method is generally on the basis of the dynamic equation including total mass, damping and stiffness matrices. In such a case the calculation is time-consuming for the system including large number of degrees-of-freedom. Therefore, compare to the aforementioned time-domain method, the computational time of the proposed frequency-domain method is significantly reduced although the time history analysis is involved.

Besides Yu and Zhou (2008), the dynamic response of structure equipped with supplemental dampers is studied by Singh (1990) and Song et al. (2008). Singh (1980) presented a method using state-vector to estimate the modal damping so that the classical modal analysis approach and square-root-of-the-sum-of-the-squares (SRSS) procedures can be adopted. Song et al. (2008) developed a systematic approach for seismic analysis of structures equipped considering non-classical damping and over-damped modes. In their study, a novel transformation matrix is firstly established to decouple the dynamic equation. Then, two modal combination rules that are applicable for non-classical damping and overdamped modes are presented to superposition the modal responses. It is worth pointing out that the earthquake input models in the present paper and Song's work are different. For the analysis considering multi-support earthquake excitations, the acceleration input model is more convenient because the most earthquake histories are in terms of acceleration. However, the displacement input model adopted in Song's paper has the advantage that the coupled damping is included in the total damping matrix and does not appear in the dynamic equation. In fact, the methods in the present paper and Song's work are essentially the same but focus on different key points.

5 Numerical example and verification

It is assumed that the soil conditions of different supports are identical in the numerical example. El Centro and Tianjin earthquake acceleration histories recorded at firm- and soft-soil conditions are selected as ground motion inputs, respectively. It should be noted that the earthquake velocity and displacement histories used in this paper can be attained by integrating the earthquake acceleration record. The acceleration, velocity and displacement histories of different earthquakes are given in Figs. 2 and 3, and the peak ground acceleration, velocity and displacement are highlighted.

The typical structures originally taken from references (Clough and Penzien 1993; Yu and Zhou 2008) are given as follows. As shown in Fig. 4, a 10 ft long rigid bar which has additional lumped mass $m/2$ at each end is considered in both structures A and B, and the total uniformly distributed mass of the bar is m. This bar is rigidly attached to the top of a weightless column of length L and there is a lateral spring support at mid-height of the bar. Without considering the supplemental damper, the overall mass and stiffness matrices can be given as follows

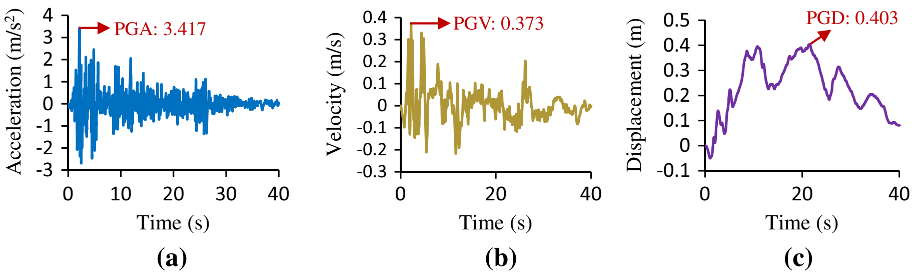

Fig. 2 Acceleration, velocity and displacement histories of El Centro earthquake. **a** Acceleration history, **b** Velocity history, **c** Displacement history. *Asterisk* PGA, PGV and PGD represent the peak ground acceleration, velocity and displacement, respectively

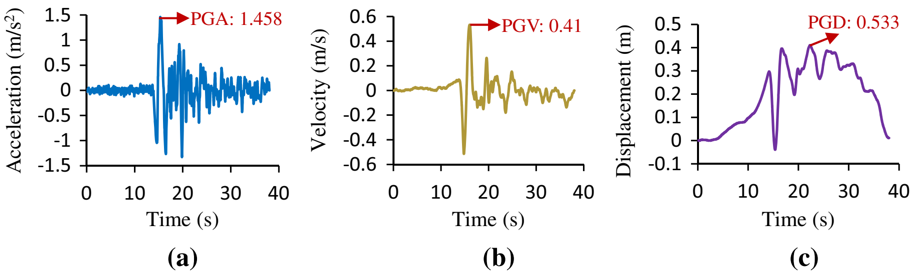

Fig. 3 Acceleration, velocity and displacement histories of Tianjin earthquake. **a** Acceleration history, **b** Velocity history, **c** Displacement history. *Asterisk* PGA, PGV and PGD represent the peak ground acceleration, velocity and displacement, respectively

$$\boldsymbol{M}_{total} = \begin{bmatrix} \boldsymbol{M} & \boldsymbol{M}_c \\ \boldsymbol{M}_c^T & \boldsymbol{M}_g \end{bmatrix} = \frac{m}{6}\begin{bmatrix} 5 & 1 & 0 & 0 \\ 1 & 5 & 0 & 0 \\ 0 & 0 & \frac{6m_a}{m} & 0 \\ 0 & 0 & 0 & \frac{6m_b}{m} \end{bmatrix} \tag{41}$$

$$\boldsymbol{K}_{total} = \begin{bmatrix} \boldsymbol{K} & \boldsymbol{K}_c \\ \boldsymbol{K}_c^T & \boldsymbol{K}_g \end{bmatrix} = \frac{EI}{L^3}\begin{bmatrix} 30.5 & -7.5 & -5 & -18 \\ -7.5 & 6.5 & -5 & 6 \\ -5 & -5 & 10 & 0 \\ -18 & 6 & 0 & 12 \end{bmatrix} \tag{42}$$

where $m = 5833.61$ kg/m; $EI/L^3 = 43{,}752.07$ N/m; m_a and m_b are the lumped mass of support a and b, respectively; $\boldsymbol{M}_{total}$ and $\boldsymbol{K}_{total}$ are the overall mass and stiffness matrices, respectively. As shown in Fig. 4, y_1 and y_2 are the displacements of nodes 1 and 2, respectively; u_{ga} and u_{gb} are the displacements of supports a and b, respectively.

Initially, the damping matrix $\boldsymbol{C}_{total}$ is assigned following the Rayleigh rule

$$\begin{aligned}\boldsymbol{C}_{total} =& \alpha\boldsymbol{M}_{total} + \beta\boldsymbol{K}_{total}\\ =&0.2\times\frac{m}{6}\begin{bmatrix}5 & 1 & 0 & 0\\ 1 & 5 & 0 & 0\\ 0 & 0 & \frac{6m_a}{m} & 0\\ 0 & 0 & 0 & \frac{6m_b}{m}\end{bmatrix} + 0.00173\times\frac{EI}{L^3}\begin{bmatrix}30.5 & -7.5 & -5 & -18\\ -7.5 & 6.5 & -5 & 6\\ -5 & -5 & 10 & 0\\ -18 & 6 & 0 & 12\end{bmatrix}\\ =&\begin{bmatrix}3280.8 & -373.23 & -379.18 & -1362.15\\ -373.23 & 1464.3 & -379.18 & 453.56\\ -379.18 & -379.18 & 756.91+3m_a & 0\\ -1362.15 & 453.56 & 0 & 908.58+3m_b\end{bmatrix}\end{aligned} \tag{43}$$

where $\alpha = 0.2(s^{-1})$, $\beta = 0.00173(s)$.

The typical structure can be transformed into a non-proportionally damped system by equipping a supplemental damper on the structure. The concentrated damper in Fig. 4a is assigned at node 1, which is consistent with the damper arrangement of the numerical example in Yu's paper (2008). In this case, stiffness and damping matrices of structure A are given as follows

$$\boldsymbol{K}'_{total} = \frac{EI}{L^3}\begin{bmatrix}30.05+k & -7.5 & -5 & -18\\ -7.5 & 6.5 & -5 & 6\\ -5 & -5 & 10 & 0\\ -18 & 6 & 0 & 12\end{bmatrix} \tag{44}$$

$$\boldsymbol{C}'_{total} = \begin{bmatrix}3280.8+c & -373.23 & -379.18 & -1362.15\\ -373.23 & 1464.3 & -379.18 & 453.56\\ -379.18 & -379.18 & 756.91+3m_a & 0\\ -1362.15 & 453.56 & 0 & 908.58+3m_b\end{bmatrix} \tag{45}$$

where k and c represent the increments of stiffness and damping matrices produced by the concentrated damper; $\boldsymbol{K}'_{total}$ and $\boldsymbol{C}'_{total}$ are the overall stiffness and damping matrices of structure A. It is noted that only the diagonal elements of the damping matrix are changed by the supplemental concentrated damper while the off-diagonal elements in $\boldsymbol{C}'_{total}$ remain unchanged.

As illustrated in Fig. 4b, the supplemental coupled damper is assigned between node 1 and support b. Clearly, not only the diagonal elements but also the off-diagonal elements of the stiffness and damping matrices have been changed. It is debatable that the coupled damping in Eq. (7) can be ignored in this case. The stiffness and damping matrices of structure B can be written in the following form

$$K''_{total} = \frac{EI}{L^3}\begin{bmatrix}30.5+k & -7.5 & -5 & -18+k\\ -7.5 & 6.5 & -5 & 6\\ -5 & -5 & 10 & 0\\ -18+k & 6 & 0 & 12+k\end{bmatrix} \tag{46}$$

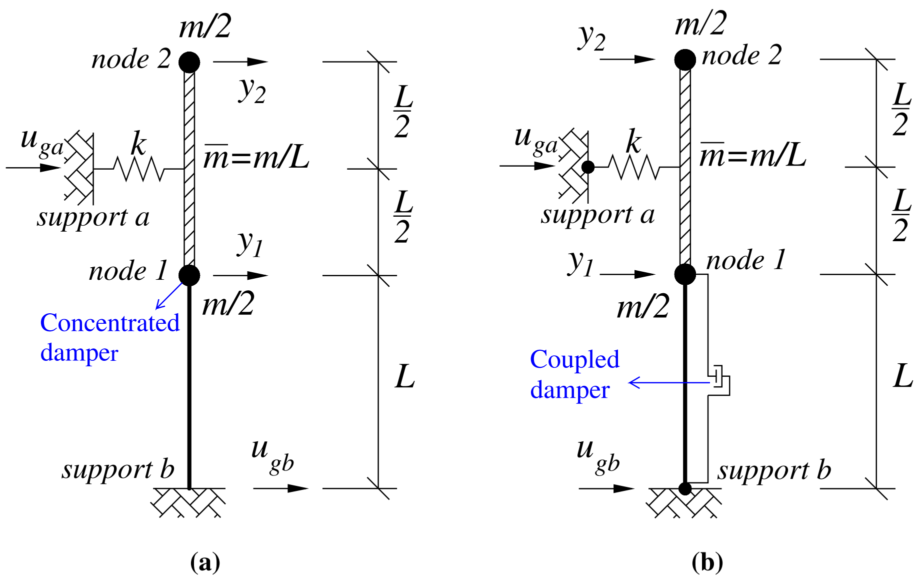

Fig. 4 Typical structures. **a** Structure A, **b** Structure B (with a concentrated damper at node 1) (with a coupled damper between node 1 and support b)

$$C''_{total} = \begin{bmatrix} 3280.8 + c & -373.23 & -379.18 & -1362.15 + c \\ -373.23 & 1464.3 & -379.18 & 453.56 \\ -379.18 & -379.18 & 756.91 + 3m_a & 0 \\ -1362.15 + c & 453.56 & 0 & 908.58 + 3m_b + c \end{bmatrix} \tag{47}$$

where k and c represent the increments of stiffness and damping matrices produced by the coupled damper; $\boldsymbol{K}''_{total}$ and $\boldsymbol{C}''_{total}$ are the overall stiffness and damping matrices of structure B. Obviously, the non-diagonal elements in the total damping matrix represent the coupled damping between different nodes. It is noted that the coupled dampings between Node *1* and Support *b* (denoted by $\boldsymbol{C}''_{total}(1,4)$ and $\boldsymbol{C}''_{total}(4,1)$) are changed due to the supplemental coupled damper. This is how the coupled damping is modeled.

The calculation process of the improved CMSRS method under certain earthquake excitation is given in Fig. 5. The detailed calculation process of the conventional CMSRS method is expounded by Yu and Zhou (2008).

The maximum displacements of structures A and B calculated by conventional and improved CMSRS methods under El Centro seismic excitation are listed in Table 2. Moreover, a series of damping increments produced by the supplemental damper are considered.

The numerical analysis agrees with the fact that the displacements of the structures decrease with the increasing damping. Moreover, the maximum displacements calculated by conventional and improved CMSRS methods are almost the same for structure. However, as for structure B, the results calculated by improved CMSRS method are significantly smaller than those calculated by conventional CMSRS method. The relative deviation between the results calculated by two methods are significantly large due to the increase of damping increment and the maximum displacement errors reach 21.2 % (at

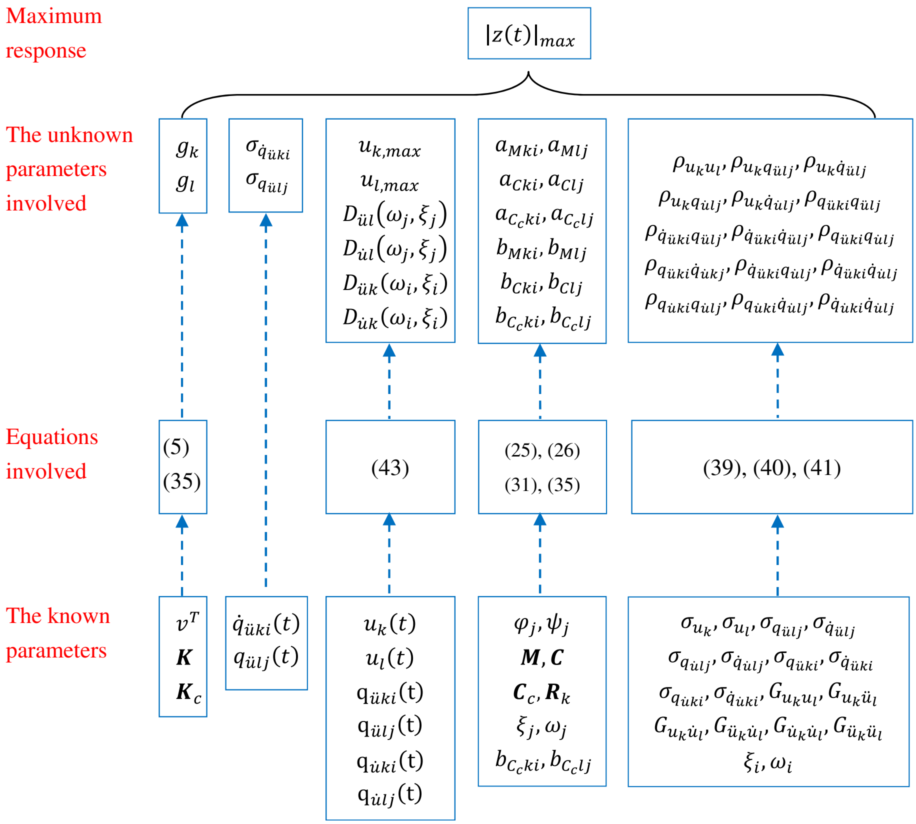

Fig. 5 The calculation flowchart for the maximum response

node 1) and 26.1 % (at node 2). Obviously, the coupled damping has a major effect on the dynamic response of the structure equipped with the coupled damper, e.g., viscoelastic damper and laminated rubber bearing.

It is necessary to point out that the maximum displacement of structure A corresponding to 40 × 3280.8 N/m/s damping increment is also calculated by Yu and Zhou (2008) based on conventional CMSRS method. However, the results in Yu's paper are different from those in this paper. It is not difficult to find that the displacement input amplitudes ($u_{k,max}$) is not given in Yu's paper (2008). If the amplitude of El Centro acceleration history is set equal to 5.88 m/s^2 (0.6 g), the computational results (0.6048 and 0.5986 m) are very similar to Yu's results (0.5980 and 0.5906 m). In order to explain the calculation process in details, the involved parameters corresponding to 40 × 3280.8 N/m/s damping increment are given in Tables 3 and 4.

In order to further analysis the mechanism of coupled damping effect on the structural dynamic response, Fig. 6 is given as follows.

In order to further compare the effects of coupled damping on the structural dynamic response under different seismic excitations, Tianjin earthquake motion recorded at soft-soil condition is taken as the seismic excitation. The maximum displacements response of structures A and B under Tianjin earthquake excitation are listed in Table 5. For structure

Table 2 Displacement error comparison of structure A and B under El Centro seismic excitation

Damping increment (N/m/s)	Response	Max displacement calculated by CMSRS method					
		Structure A			Structure B		
		Conventional	Improved	Error (%)	Conventional	Improved	Error (%)
20 × 3280.8*	y_1	0.3894	0.3894	0	0.3894	0.3758	3.6
30 × 3280.8	y_1	0.3830	0.3829	0.03	0.3830	0.3629	5.5
40 × 3280.8	y_1	0.3767	0.3767	0	0.3767	0.3504	7.5
50 × 3280.8	y_1	0.3714	0.3724	0.27	0.3714	0.3404	9.1
60 × 3280.8	y_1	0.3650	0.3654	0.11	0.3650	0.3266	11.8
100 × 3280.8	y_1	0.3431	0.3436	0.15	0.3431	0.2832	21.2
20 × 3280.8	y_2	0.3878	0.3873	0.12	0.3878	0.3716	4.4
30 × 3280.8	y_2	0.3801	0.3799	0.05	0.3801	0.3567	6.6
40 × 3280.8	y_2	0.3728	0.3727	0.02	0.3728	0.3423	8.9
50 × 3280.8	y_2	0.3666	0.3666	0	0.3666	0.3299	11.1
60 × 3280.8	y_2	0.3587	0.3596	0.25	0.3587	0.3148	14.0
100 × 3280.8	y_2	0.3339	0.3345	0.18	0.3339	0.2648	26.1

* The number 3280.8 in the first column is equal to the value of $\boldsymbol{C}_{total}(1,1)$. The value of damping increment is an integer multiple of $\boldsymbol{C}_{total}(1,1)$

Table 3 Parameters involved in conventional CMSRS method corresponding to 40 × 3280.8 damping increment

$\rho_{u_k u_l} = \begin{bmatrix} 1 & 1 \\ 1 & 1 \end{bmatrix}$	$\rho_{\dot{q}_{\ddot{u}ki}\dot{q}_{\ddot{u}lj}} = \begin{bmatrix} 1 & 0.0864 \\ 0.0864 & 1 \end{bmatrix}$	$u_{k,max} = 0.4030$
		$u_{l,max} = 0.4030$
$\rho_{u_k q_{\ddot{u}lj}} = \begin{bmatrix} 0.0548 & 0.0859 \\ 0.0548 & 0.0859 \end{bmatrix}$	$a_{M11} = (0.0192,\ -0.2051)$	$\mathrm{D}_{\ddot{u}k} = (0.0143 \quad 0.0010)$
	$a_{M12} = (0.0973,\ -0.0469)$	$\mathrm{D}_{\ddot{u}l} = (0.0143 \quad 0.0010)$
$\rho_{u_k \dot{q}_{\ddot{u}lj}} = \begin{bmatrix} 0.0504 & 0.0453 \\ 0.0504 & 0.0453 \end{bmatrix}$	$a_{M21} = (-0.0049,\ 0.0614)$	$\omega = (6.5321, 17.3322)$
	$a_{M22} = (-0.0949,\ 0.0838)$	$\xi = (0.1548, 0.7831)$
$\rho_{q_{\ddot{u}ki} q_{\ddot{u}lj}} = \begin{bmatrix} 1 & 0.2923 \\ 0.2923 & 1 \end{bmatrix}$	$b_{M11} = (0.0178,\ 0.0340)$	
	$b_{M12} = (0.0345,\ -0.0223)$	
$\rho_{\dot{q}_{\ddot{u}ki} q_{\ddot{u}lj}} = \begin{bmatrix} 0 & 0.6657 \\ -0.3816 & 0 \end{bmatrix}$	$b_{M21} = (-0.0057,\ -0.0020)$	
	$b_{M22} = (0.0026,\ 0.0125)$	

A, no matter which seismic excitation is adopted, the maximum displacements calculated by the conventional and improved CMSRS methods are almost the same, suggesting that both conventional and improved CMSRS methods are reasonable and acceptable for the dynamic analysis of structure A. However, for structure B, the displacements calculated by the improved CMSRS method are significantly less than that calculated by the

Table 4 Parameters involved in improved CMSRS method corresponding to 40 × 3280.8 damping increment

$\rho_{u_k u_l} = \begin{bmatrix} 1 & 1 \\ 1 & 1 \end{bmatrix}$	$\rho_{u_k \dot{q}_{\dot{u}kj}} = \begin{bmatrix} -0.0426 & -0.0672 \\ -0.0426 & -0.0672 \end{bmatrix}$	$b_{C21} = (-0.0242, 0.1535)$ $b_{C22} = (0.2583, 0.1497)$
$\rho_{u_k q_{\ddot{u}lj}} = \begin{bmatrix} 0.0548 & 0.0859 \\ 0.0548 & 0.0859 \end{bmatrix}$	$\rho_{q_{\ddot{u}ki} \dot{q}_{\ddot{u}lj}} = \begin{bmatrix} 0 & -0.3873 \\ 0.3873 & 0 \end{bmatrix}$	$a_{C_c 11} = (-0.0011, 0.0110)$ $a_{C_c 12} = (-0.0004, -0.0026)$
$\rho_{u_k \dot{q}_{\ddot{u}lj}} = \begin{bmatrix} 0.0504 & 0.0453 \\ 0.0504 & 0.0453 \end{bmatrix}$	$\rho_{\dot{q}_{\ddot{u}ki} \dot{q}_{\dot{u}lj}} = \begin{bmatrix} 0 & -0.6657 \\ 0.3816 & 0 \end{bmatrix}$	$a_{C_c 21} = (0.0013, -0.0144)$
$\rho_{q_{\ddot{u}ki} q_{\ddot{u}lj}} = \begin{bmatrix} 1 & 0.2923 \\ 0.2923 & 1 \end{bmatrix}$	$\rho_{q_{\dot{u}ki} \dot{q}_{\dot{u}lj}} = \begin{bmatrix} 0 & 0.1834 \\ -0.1317 & 0 \end{bmatrix}$	$a_{C_c 22} = (0.0128, -0.0096)$ $b_{C_c 11} = (-0.0009, -0.0024)$
$\rho_{\dot{q}_{\ddot{u}ki} q_{\ddot{u}lj}} = \begin{bmatrix} 0 & 0.6657 \\ -0.3816 & 0 \end{bmatrix}$	$a_{M11} = (0.0192, -0.2051)$	$b_{C_c 12} = (-0.0028, 0.0008)$ $b_{C_c 21} = (0.0013, 0.0016)$
$\rho_{\dot{q}_{\ddot{u}ki} \dot{q}_{\ddot{u}lj}} = \begin{bmatrix} 1 & 0.0864 \\ 0.0864 & 1 \end{bmatrix}$	$a_{M12} = (0.0973, -0.0469)$ $a_{M21} = (-0.0049, 0.0614)$	$b_{C_c 22} = (0.0012, -0.0021)$ $D_{\dot{u}k} = \begin{pmatrix} 0.0143 & 0.0010 \end{pmatrix}$
$\rho_{u_k q_{\dot{u}kj}} = \begin{bmatrix} -0.0080 & -0.0132 \\ -0.0080 & -0.0132 \end{bmatrix}$	$a_{M22} = (-0.0949, 0.0838)$ $b_{M11} = (0.0178, 0.0340)$	$D_{\dot{u}l} = \begin{pmatrix} 0.0143 & 0.0010 \end{pmatrix}$ $D_{\ddot{u}k} = \begin{pmatrix} 0.0732 & 0.0090 \end{pmatrix}$
$\rho_{q_{\ddot{u}ki} q_{\dot{u}kj}} = \begin{bmatrix} 0 & -0.1317 \\ 0.1834 & 0 \end{bmatrix}$	$b_{M12} = (0.0345, -0.0223)$ $b_{M21} = (-0.0057, -0.0020)$	$D_{\ddot{u}l} = \begin{pmatrix} 0.0732 & 0.0090 \end{pmatrix}$ $\omega = (6.5321, 17.3322)$
$\rho_{\dot{q}_{\ddot{u}ki} q_{\dot{u}lj}} = \begin{bmatrix} 0.4358 & 0.0914 \\ 0.0729 & 0.1793 \end{bmatrix}$	$b_{M22} = (0.0026, 0.0125)$ $a_{C11} = (0.0094, 0.1174)$	$\xi = (0.1548, 0.7831)$
$\rho_{q_{\dot{u}ki} q_{\dot{u}lj}} = \begin{bmatrix} 1 & 0.9167 \\ 0.9167 & 1 \end{bmatrix}$	$a_{C12} = (-1.6638, 1.7239)$ $a_{C21} = (0.0018, 0.1804)$	
$\rho_{\dot{q}_{\dot{u}ki} \dot{q}_{\dot{u}lj}} = \begin{bmatrix} 1 & 0.2920 \\ 0.2920 & 1 \end{bmatrix}$	$a_{C22} = (-0.5601, 1.6056)$ $b_{C11} = (-0.0195, 0.1806)$	
	$b_{C12} = (0.2950, 0.1546)$	

conventional CMSRS method, and the relative deviation becomes more significant due to the increase of damping increment. Furthermore, the errors between the results calculated by the conventional and improved CMSRS methods reach 20.9 % (at node 1) and 25.8 % (at node 2).

In order to indicate the correctness of the improved CMSRS method, the dynamic response of structure B is further calculated by Newmark-β method under El Centro earthquake excitation. The integration step is set to 0.02 s and the parameters β and γ are assigned to 0.25 and 0.05, respectively.

As shown in Fig. 7, the comparison between the displacement responses calculated by the proposed frequency method and the time history method shows good agreement. Therefore, it is unreasonable and inaccurate to calculate the dynamic response of structure B by conventional CMSRS method.

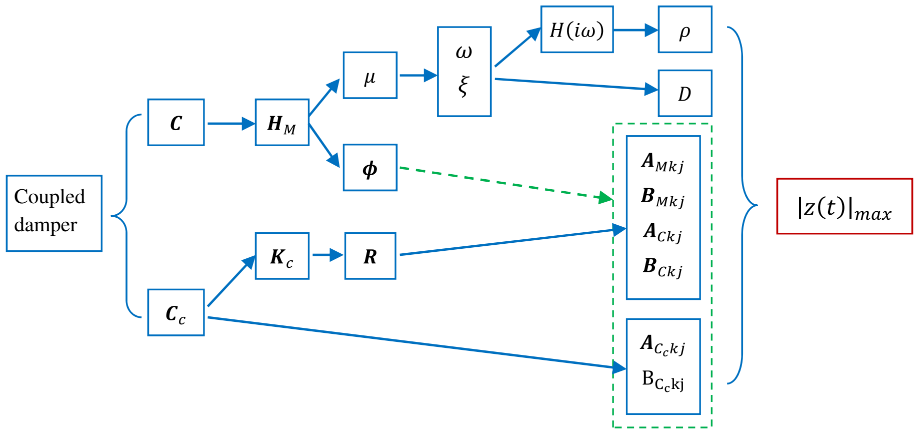

Fig. 6 Effects of coupled damping on the maximum displacement

Table 5 Displacement error comparison of structure A and B under Tianjin seismic excitation

Damping increment (N/m/s)	Response	Max displacement calculated by CMSRS method					
		Structure A			Structure B		
		Conventional	Improved	Error (%)	Conventional	Improved	Error (%)
20 × 3280.8*	y_1	0.3962	0.3961	0.03	0.3962	0.3823	3.6
30 × 3280.8	y_1	0.3896	0.3896	0	0.3896	0.3692	5.5
40 × 3280.8	y_1	0.3832	0.3832	0	0.3832	0.3564	7.5
50 × 3280.8	y_1	0.3777	0.3822	1.2	0.3777	0.3488	8.3
60 × 3280.8	y_1	0.3717	0.3717	0	0.3717	0.3335	11.5
100 × 3280.8	y_1	0.3496	0.3496	0	0.3496	0.2892	20.9
20 × 3280.8	y_2	0.3944	0.3940	0.10	0.3944	0.3781	4.8
30 × 3280.8	y_2	0.3866	0.3865	0.03	0.3866	0.3629	6.5
40 × 3280.8	y_2	0.3792	0.3791	0.03	0.3792	0.3483	8.9
50 × 3280.8	y_2	0.3728	0.3737	0.24	0.3728	0.3363	10.9
60 × 3280.8	y_2	0.3658	0.3659	0.03	0.3658	0.3217	13.7
100 × 3280.8	y_2	0.3403	0.3403	0	0.3403	0.2706	25.8

* The number 3280.8 in the first column is equal to the value of $\boldsymbol{C}_{total}(1,1)$. The value of damping increment is an integer multiple of $\boldsymbol{C}_{total}(1,1)$

Comprehensively speaking, the conventional CMSRS method is only applicable to the structure equipped with a concentrated damper. For structures equipped with the coupled damper, e.g., viscoelastic damper and laminated rubber bearing, the effect of coupled damping matrix on the structural dynamic response cannot be ignored and it is unreasonable and inaccurate to calculate the dynamic response by the conventional CMSRS method. The improved CMSRS method properly accounts for the coupled damping matrix

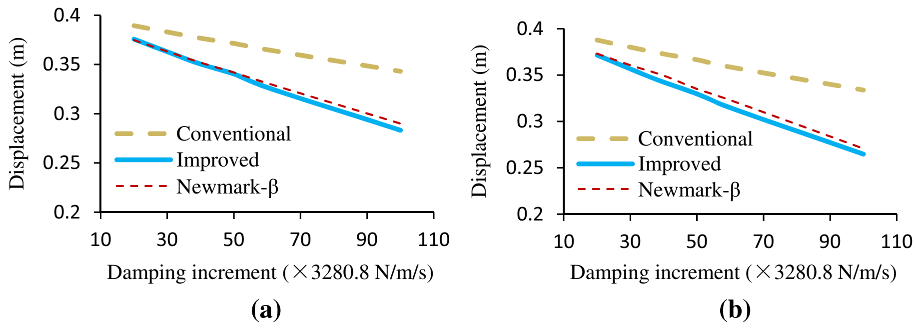

Fig. 7 Comparison among the responses of structure B calculated by different methods. **a** Displacement of Node *1*, **b** Displacement of Node *2*

in the dynamics equations and is applicable to both structures equipped with concentrated and coupled dampers.

6 Concluding remarks

It is debatable whether the coupled damping of non-classically damped linear system can be ignored in conventional CMSRS method. Therefore, the conventional CMSRS method is reconsidered and reanalyzed in detail in this paper and the main conclusions are summarized as follows:

1. An improved CMSRS method accounting for the coupled damping is deduced and proposed on the basis of conventional CMSRS method and random vibration theory. The complex mode analysis method is adopted to decouple the dynamic equation due to the nonorthogonality of the damping matrix, and the equations for structure response estimations under multiple-support seismic excitations are deduced. Nine new cross-correlation coefficients are introduced into the CMSRS formulae, thus the correlations between the modal responses under different input excitations (velocity or acceleration) are comprehensively considered.
2. A typical structure equipped with concentrated or coupled damper is taken as example to investigate the differences between the conventional and improved CMSRS methods. The El Centro and Tianjin ground motions recorded at firm- and soft-soil conditions are selected as the dynamic excitations respectively. Results indicate that the coupled damping has a slight effect on the dynamic response of the structure equipped with a concentrated damper, but for the structure equipped with a coupled damper, e.g., the viscoelastic damper or the laminated rubber bearing, unnegligible errors will be introduced if the coupled damping is ignored. Moreover, the comparison between the displacement results from the proposed frequency method and the time history method for the structure equipped with coupled damper shows good agreement. Numerical results indicate that the improved CMSRS method is more reasonable and accurate for the dynamic analysis of structures equipped with coupled damper.

Acknowledgments This work was supported by the National Natural Science Foundation of China (Grant No. 51408409) and the Tianjin Research Program of Application Foundation and Advanced Technology (Grant No. 15JCQNJC07400).

References

Alexander NA (2008) Multi-support excitation of single span bridges, using real seismic ground motion recorded at the SMART-1 array. Comput Struct 86(1–2):88–103

Allam SM, Datta TK (2000) Analysis of cable-stayed bridges under multi-component random ground motion by response spectrum method. Eng Struct 22(10):1367–1377

Berrah M, Kausel E (1992) Response spectrum analysis of structures subjected to spatially varying motion. Earthq Eng Struct Dyn 21(6):461–470

Caughey TK, O'kelly MEJ (1965) Classical normal modes in damped linear dynamic systems. J Appl Mech 32(3):583–588

Chopra AK (2001) Dynamics of structures: theory and applications to earthquake engineering, 2nd edn. Prentice Hall, Englewood Cliffs

Clough RW, Penzien J (1993) Dynamics of structures, 2nd edn. McGraw-Hill Inc, New York

Constantinou MC, Symans MD (1992) Experimental and analytical investigation of seismic response of structures with supplemental fluid viscous dampers. Research Report. National center for earthquake engineering research. SUNY at buffalo, New York

Foss FK (1958) Co-ordinates which uncouple the linear dynamic systems. J Appl Mech 25(24):361–364

Hao H (1991) Response of multiply-supported rigid plate to spatially correlated seismic excitations. Earthq Eng Struct Dyn 20(9):821–838

Hao H, Xiao ND (1995) Response of asymmetric structures to multiple ground motions. J Struct Eng 121(11):1557–1564

Hao H, Xiao ND (1996) Multiple excitation effects on response of symmetric buildings. Eng Struct 18(9):732–740

Heredia-Zavoni E, Leyva A (2003) Torsional response of symmetric buildings to incoherent and phase-delayed earthquake ground motion. Earthq Eng Struc Dyn 32(7):1021–1038

Igusa T, Kiureghian AD, Sackman JL (1984) Modal decomposition method for stationary response of non-classically damped systems. Earthq Eng Struct Dyn 12(1):121–136

Kato S, Su L (2002) Effects of surface motion difference at footings on the earthquake responses of large-span cable structures. Steel Constr Eng 9:113–128

Kato S, Nakazawa S, Su L (2003) Effects of wave passage and local site on seismic responses of a large-span reticular dome structure. Steel Constr Eng 10(37):91–106

Kiureghian AD, Neumnhofer A (1992) A response spectrum method for multiple-support seismic excitations. Earthq Eng Struct Dyn 21(8):713–740

Liang Z, Lee GC (2013) Towards multiple hazard resilient bridges: a methodology for modeling frequent and infrequent time-varying loads Part II, Examples for live and earthquake load effects. Earthq Eng Eng Vib 11(3):303–311

Liang Z, Lee GC, Dargush GF, Song J (2012) Structural damping: applications in seismic response modification. CRC Press, Florida

Lou CH, Ku BD (1995) An efficient analysis of structural response for multiple-support seismic excitations. Eng Struct 17(1):15–26

Maldonado GO, Singh MP (1991) An improved response spectrum method for seismic design response. Part 2: non-classically damped structures. Earthq Eng Struct Dyn 20(7):637–649

Rutenberg A, Heidebrecht AC (1987) Approximate spectral multiple-support seismic analysis; traveling wave approach. Research Report. Department of Civil Engineering, McMaster Univesity, Hamilton

Singh M (1980) Seismic response by SRSS for nonproportional damping. J Eng Mech Div 106(6):1405–1419

Song J, Liang Z, Chu YL, Lee GC (2007) Peak earthquake response of structures under multi-component excitations. Earthq Eng Eng Vib 6(4):354–370

Song J, Chu YL, Liang Z, Lee GC (2008) Modal analysis of generally damped linear structures subjected to seismic excitations. Technical Report. Multidisciplinary center for earthquake engineering research MCEER. SUNY at buffalo, New York

Su L, Dong SL, Kato S (2006) A new average response spectrum method for linear response analysis of structures to spatial earthquake ground motions. Eng Struct 28(13):1835–1842

Yamamura N, Tanaka H (1990) Response analysis of flexible MDOF system for multiple-support seismic excitations. Earthq Eng Struct Dyn 19:345–357

Yao GF, Gao XF (2011) Controllability of regular systems and defective systems with repeated eigenvalues. J Vib Control 17(10):1574–1581

Yu RF, Zhou XY (2008) Response spectrum analysis for non-classically damped linear system with multiple-support excitations. Bull Earthq Eng 6(2):261–284

Yu RF, Zhou XY, Yuan MQ (2012) Dynamic Response Analysis of Generally Damped Linear System with Repeated Eigenvalues. Struct Eng Mech 42:449–469

Zerva A (1990) Response of multi-span beams to spatially incoherent seismic ground motions. Earthq Eng Struct Dyn 19(6):819–832

Zhang ZC, Lin JH, Zhang YH, Zhao Y, Howsonc WP, Williams FW (2010) Non-stationary random vibration analysis for train–bridge systems subjected to horizontal earthquakes. Eng Struct 32(11):3571–3582

Zhou XY, Yu RF, Dong D (2004) Complex mode superposition algorithm for seismic responses of non-classically damped linear system. J Earthq Eng 8(4):597–641